Linearity Limits of the Varactor-Controlled Osc–Mod Circuits

DARKO KAJFEZ, SENIOR MEMBER, IEEE, AND EUGENE J. HWAN, MEMBER, IEEE

Abstract —A method for optimum selection of the natural frequencies of a varactor-controlled oscillator (osc–mod) is developed for the purpose of providing the best modulation linearity, while still retaining practical features such as continuous tuning. Highly linear operation was found to be possible using conventional abrupt varactors if the circuit has one pole and two zeros situated below the operating frequency. The limits of the maximum realizable modulation bandwidths are established for a linearity of one percent, with and without the requirement for continuous tuning.

I. Introduction

THE OSCILLATOR–MODULATOR (osc–mod) is a special case of the voltage-controlled oscillator used for generating the FM signal in microwave communications equipment. Three specific requirements make the osc–mod different from other VCO's: 1) strict linearity in a relatively narrow range of frequencies, 2) very low noise, and 3) high efficiency.

A variety of different osc–mod circuits have been described (see, e.g., [1]–[10]). This paper addresses the first of the three topics listed above: the linearization of the varactor-controlled osc–mod. The analysis is intended to be general and is not limited to a specific circuit. The general approach is achieved by describing the osc–mod circuit in terms of the natural frequencies of a lossless two-port when one of its ports is short circuited. The goal is to establish the theoretical performance limits which can be used as design guidelines.

II. Normalized Modulation Curve

Fig. 1 shows the general osc–mod equivalent circuit which is used in the present analysis. Port 1 is the reference plane of the active device maintaining the oscillations, and port 2 is a varactor junction which is utilized to modulate the oscillation frequency. Between these two nonlinear semiconductor devices is a linear two-port incorporating one or several resonant circuits, package elements, mechanical tuning devices, sections of transmission lines, and various parasitic elements. The baseband modulation voltage is brought to the osc–mod at port 3 and the RF output power is taken from port 4. To simplify the analysis, it will be assumed that the two-port is lossless.

Manuscript received September 20, 1984; revised February 25, 1985. The work described in this paper was performed at Farinon Division.
D. Kajfez is with the Department of Electrical Engineering, University of Mississippi, University, MS 38677.
E. J. Hwan is with Harris Corp., Farinon Division, 1691 Bayport Ave., San Carlos, CA 94070.

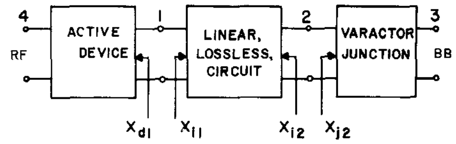

Fig. 1. Osc–mod block diagram.

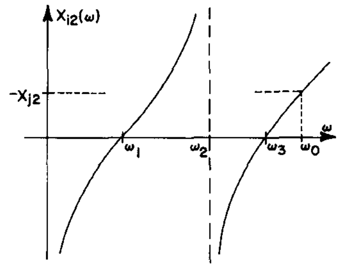

Fig. 2. Reactance of a lossless network.

For the osc–mod described in Section VI, the active device at port 1 is the base terminal of a microwave bipolar transistor. The oscillations occur at the frequency at which the reactance X_{l1}, "seen" by the active device, is passing through series resonance. The oscillation frequency ω_0 can thus be determined from the condition $X_{l1}(\omega_0)=0$. Neglecting the real parts of the impedances at both ports, the oscillation frequency can also be found from the following condition:

$$X_{l2}(\omega_0) = -X_{j2}(\omega_0) \tag{1}$$

where X_{l2} is the reactance "seen" by the varactor junction when port 1 is short circuited, and X_{j2} is the reactance of the varactor junction. The reactance X_{l2} can be expressed by Foster's theorem in terms of poles and zeros. For instance, if the poles occur at the origin and at ω_2 while the zeros occur at ω_1 and ω_3 as in Fig. 2, the reactance Z_{l2} is

$$X_{l2}(\omega) = K\frac{(\omega^2-\omega_1^2)(\omega^2-\omega_3^2)}{\omega(\omega^2-\omega_2^2)}. \tag{2}$$

As seen in Fig. 2, the oscillation frequency ω_0 is the one at which (1) is satisfied.

The varactor junction capacitance can be expressed as

$$X_{j2} = -\frac{(V_b+\phi_c)^\alpha}{\omega C_{j0}}. \tag{3}$$

V_b is the reverse bias voltage, ϕ_c is the contact potential, and C_{j0} is the junction capacitance at $V_b+\phi_c = 1$ V. The

0018-9480/85/0700-0620$01.00 ©1985 IEEE

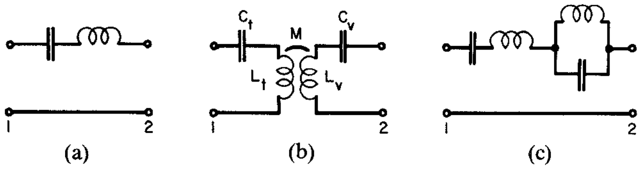

Fig. 3. Possible realizations of osc–mod two-ports.

bias voltage consists of the constant part V_{b0} and of the modulation voltage V_m. The normalized modulation voltage is then denoted by v

$$v = \frac{V_m}{V_{b0} + \phi_c}. \tag{4}$$

When $\omega = \omega_0$, $v = 0$. This leads to

$$1 + v = \left[\frac{(\omega^2 - \omega_1^2)(\omega_0^2 - \omega_2^2)(\omega^2 - \omega_3^2)}{(\omega_0^2 - \omega_1^2)(\omega^2 - \omega_2^2)(\omega_0^2 - \omega_3^2)} \right]^{1/\alpha}.$$

It is convenient to normalize, also, the frequency as follows:

$$\frac{\omega_i}{\omega_0} = \Omega_i \qquad \text{for } i = 1,2,3. \tag{5}$$

In the vicinity of the operating point, the normalized frequency is

$$\frac{\omega}{\omega_0} = 1 + \eta \tag{6}$$

where $\eta = (\omega - \omega_0)/\omega_0$ is the normalized frequency change (a very small number). The modulation curve is then brought to its normalized form

$$1 + v = \left[\frac{(1+\eta)^2 - \Omega_1^2}{1 - \Omega_1^2} \cdot \frac{1 - \Omega_2^2}{(1+\eta)^2 - \Omega_2^2} \cdot \frac{(1+\eta)^2 - \Omega_3^2}{1 - \Omega_3^2} \right]^{1/\alpha}. \tag{7}$$

If the lossless circuit between the varactor junction and the transistor base has more than three finite natural frequencies, expression (7) can be easily expanded to include any additional zeros and poles. The conceptual advantage of using the block diagram from Fig. 1 is describing the modulation curve in terms of (normalized) poles and zeros, irrespective of any particular circuit diagram.

III. Single Resonator

The simplest possible two-port between the varactor and the active device is a single series resonant circuit shown in Fig. 3(a). The modulation curve (7) simplifies to

$$1 + v = \left[1 + A_1 \eta + \frac{A_1}{2} \eta^2 \right]^{1/\alpha}. \tag{8}$$

The constant A_1 is an abbreviation for

$$A_1 = \frac{2}{1 - \Omega_1^2}. \tag{9}$$

Since η is a small number, it is convenient to use the binomial expansion to obtain first two terms of the Taylor series for v as follows:

$$v = C_1 \eta + C_2 \eta^2. \tag{10}$$

The constants C_1 and C_2 are

$$C_1 = \frac{A_1}{\alpha} \tag{11}$$

$$C_2 = \frac{A_1}{2^\alpha} \left[1 + \left(\frac{1}{\alpha} - 1 \right) A_1 \right]. \tag{12}$$

The slope coefficient C_1 is the inverse of the normalized sensitivity S_n

$$S_n = \left. \frac{d\eta}{dv} \right|_{\omega_0} = S \cdot \frac{V_{b+}\phi_c}{f_0} \tag{13}$$

where S is the actual sensitivity in hertz per volt. Thus, the normalized sensitivity of the circuit in Fig. 3(a) must satisfy the following equation:

$$S_n = \frac{\alpha}{2}(1 - \Omega_1^2). \tag{14}$$

The required value of S_n is typically a small number: at $f_0 = 2$ GHz, a sensitivity $S = 4$ MHz/V for a varactor operating at $V_b + \phi_c = 10$ V gives the value of $S_n = 0.02$.

The modulation curve is linearized by requesting $C_2 = 0$. This leads to

$$\alpha = \frac{2}{1 + \Omega_1^2}. \tag{15}$$

Since $\Omega_1 < 1$, α must be larger than unity. Therefore, the only possible way to linearize the modulation curve for a circuit consisting of a single resonator is to use a hyperabrupt varactor. Equations (14) and (15) can be used as design expressions for choosing a correct varactor α for a specified S_n. As an example, for $S_n = 0.02$, the required varactor exponent is $\alpha \simeq 1.02$. Even though hyperabrupt varactors with a specific exponent are available, the single-resonator circuit does not provide sufficient flexibility to accommodate small variations in α. The circuit described in the next section offers more degrees of freedom.

IV. Two Coupled Resonators

Several authors ([1]–[4]) have shown that when the osc–mod consists of two coupled resonant circuits, it is possible to linearize the modulation curve by using conventional varactors with $\alpha < 1$. For the inductively coupled pair of lumped resonant circuits in Fig. 3(b), the position of natural frequencies ω_1, ω_2, and ω_3 (when port 2 is short-circuited) is such as shown in Fig. 2. The circuit reactance X_{i2} is a growing function of frequency displaying two zeros denoted ω_1 and ω_3 and one pole denoted ω_2. In order to achieve resonance with the varactor junction capacitance, reactance X_{i2} must be positive. Therefore, the operating frequency ω_0 is situated above the zero ω_3.

The linearity of the modulation curve for the circuit consisting of two resonators can be studied by expanding (7) in a three-term Taylor series

$$v = C_1 \eta + C_2 \eta^2 + C_3 \eta^3. \tag{16}$$

Using the notation from (9)

$$A_i = \frac{2}{1 - \Omega_i^2} \qquad \text{for } i = 1,2,3 \tag{17}$$

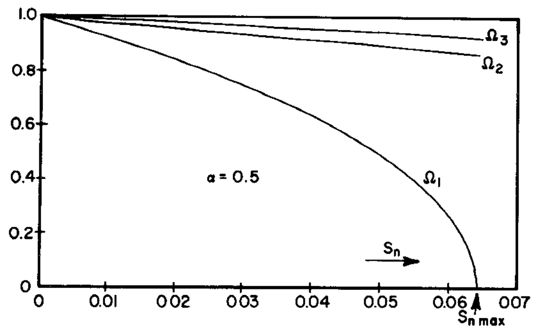

Fig. 4. Optimum position of natural frequencies for $C_2 = C_3 = 0$, $\alpha = 0.5$.

the coefficients in Taylor's expansion are expressed as follows:

$$C_1 = \frac{1}{\alpha}(A_1 - A_2 + A_3) \tag{18}$$

$$C_2 = \frac{1}{2}\left[C_1 + C_1^2 - \frac{1}{\alpha}(A_1^2 - A_2^2 + A_3^2)\right] \tag{19}$$

$$C_3 = -\frac{C_1^3}{3} - \frac{C_1^2}{2} - \frac{C_1}{2} + C_2\left(\frac{1}{2} + C_1\right) + \frac{1}{3\alpha}(A_1^3 - A_2^3 + A_3^3). \tag{20}$$

The normalized sensitivity at the center frequency S_{n0} is usually specified at the outset of the design. Since $S_{n0} = 1/C_1$, we obtain from (18)

$$A_1 - A_2 + A_3 = \frac{\alpha}{S_{n0}}. \tag{21}$$

The linearity of the modulation curve requires $C_2 = 0$. This results in

$$A_1^2 - A_2^2 + A_3^2 = \frac{\alpha}{S_{n0}}\left(1 + \frac{1}{S_{n0}}\right). \tag{22}$$

Since there are three natural frequencies to be selected, it is possible to introduce the additional requirement $C_3 = 0$, obtaining the following equation:

$$A_1^3 - A_2^3 + A_3^3 = \frac{\alpha}{S_{n0}}\left[\frac{3}{2} + \frac{1}{S_{n0}}\left(\frac{3}{2} + \frac{1}{S_{n0}}\right)\right]. \tag{23}$$

The above three nonlinear equations must be solved numerically in order to find the optimum position of natural frequencies which force both the second and third coefficient in the modulation curve (16) to vanish. For the abrupt junction varactors with $\alpha = 0.5$, the results of the numerical solutions are shown in Fig. 4.

The calculated values Ω_1, Ω_2, and Ω_3 can now be substituted in (7), and the relative frequency η can be gradually varied so that the normalized modulation curve $v(\eta)$ is evaluated. Instead of plotting this curve, the sensitivity versus frequency has been computed by numerical differentiation and plotted in Fig. 5. Three different values of the normalized sensitivity are shown: $S_{n0} = 0.01$, 0.02, and 0.03. Using the data computed in such a manner, it is possible to read the values Ω_L and Ω_U for which the sensitivity S_n departs one percent from its nominal value S_{n0}. The corresponding relative bandwidths

$$\Delta\Omega = \Omega_U - \Omega_L$$

are summarized in Table I.

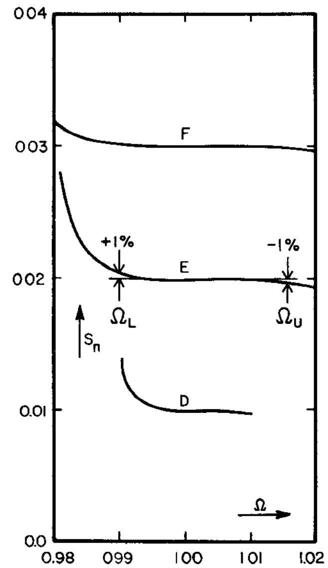

Fig. 5. Normalized modulation curves for the natural frequencies from Fig. 4. Curve D: $S_{n0} = 0.01$, Curve E: $S_{n0} = 0.02$, Curve F: $S_{n0} = 0.03$.

TABLE I

S_{n0}	$\Delta\Omega$ (1%) (Fig. 5)	$\Delta\Omega$ (1%) (Fig. 9)
0.01	0.0109	0.0049
0.02	0.0214	0.0108
0.03	0.0319	0.0191

It is seen that the sensitivity curves are S-shaped because the first and the second derivatives of sensitivity are zero. It is further seen that the higher the chosen value of S_{n0}, the wider the bandwidth within which the departure from linearity stays within prescribed limits. For instance, for 1 percent departure from linearity, the sensitivity $S_{n0} = 0.02$ results in the relative bandwidth of 0.0214, while for $S_{n0} = 0.03$ the relative bandwidth is 0.0319. These are optimum values that can be achieved with a circuit which has three finite natural frequencies as shown in Fig. 2. This is true for any two-port with natural frequencies as shown in Fig. 2. For example, Aitchison and Gelsthorpe [7] have shown that the circuit shown in Fig. 3(c) is also well-suited for linearization of a voltage-controlled oscillator.

Starting from the prescribed values of optimal frequencies, it is possible to synthesize the two-port lumped elements. As an example, suppose the sensitivity $S = 3$ MHz/V is desired at a carrier frequency of 1.75 GHz. The varactor has $\phi_c = 0.7$ V, $\alpha = 0.5$, and 1.4-pF junction capacitance at $V_{b0} = 10$ V. Using the natural frequencies from Fig. 4, the element values for the lumped circuit in Fig. 3(b) are obtained as follows: $L_v = 37.5$ nH, $C_v = 0.291$ pF, $M = 0.594$ nH, $L_t = 1.4$ nH, $C_t = 6.42$ pF.

V. Continuity of Tuning

At microwave frequencies, varactor Q is moderately low so that the varactor junction in Fig. 1 must be modeled by a series combination of the capacitance C_j and resistance

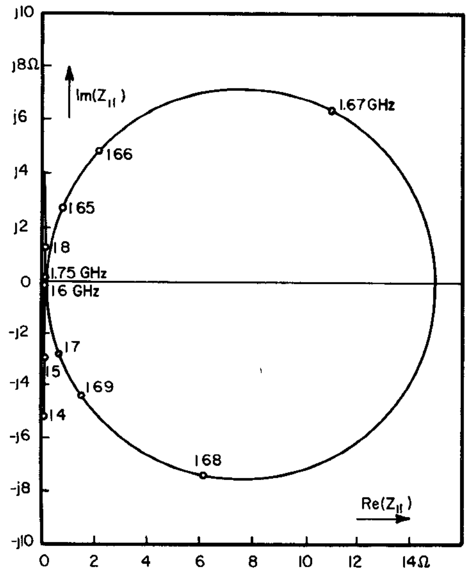

Fig. 6. Impedance Z_{i1} of the circuit from Fig. 3(b) ($C_2 = C_3 = 0$).

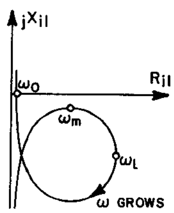

Fig. 7. The loop of the impedance Z_{i1} is situated below the real axis.

R_s. For $Q_v = 25$ at the bias of 10 V, the resistance in the circuit from the previous example is $R_s = 2.6\ \Omega$. Even though the two-port between ports 1 and 2 is lossless, the input impedance Z_{i1} "seen" by the active device has a nonvanishing real part. For the circuit in the above example, the computed input impedance is shown in Fig. 6.

The reactance passes through zero at 1.75 GHz as required for the operation of the oscillator. Unfortunately, the impedance forms a loop on the complex plane at frequencies below 1.75 GHz. Such a loop has an undesired property as far as the active device is concerned: it is possible for the oscillation frequency to jump from 1.75 GHz to about 1.6 GHz where another series resonance occurs, and the reactance passes through zero again. In view of Kurokawa's graphical interpretation [11] of oscillation conditions, the frequency jump can be prevented by moving the loop below the real axis so that there will be only one intersection of the load line $Z_{i1}(\omega)$ and the device line (here, the device line coincides with the real axis). The desired behavior of $Z_{i1}(\omega)$ is shown in Fig. 7.

The loop will be located below the real axis when the following approximate condition is satisfied for the circuit in Fig. 3(b):

$$\Omega_2^2 \geq \Omega_l^2 \left(1 + \frac{k^2 Q_v \Omega_l}{2\Omega_j^2} \right). \tag{24}$$

The derivation of this condition is given in the Appendix. $\Omega_2 = \omega_2/\omega_0$ is the normalized frequency of the pole from Fig. 2, and $\Omega_l = \omega_l/\omega_0$ is the normalized resonant frequency

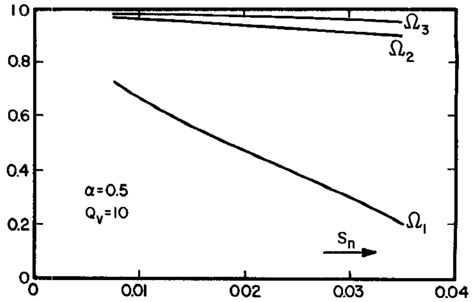

Fig. 8. Optimum position of natural frequencies for $\alpha = 0.5$ and $Q_v = 10$, satisfying the condition for continuous tuning.

of the resonant circuit on the varactor side when the varactor is added

$$\omega_l = \sqrt{\frac{C_v + C_j}{L_v C_v C_j}}. \tag{25}$$

$\Omega_j = \omega_j/\omega_0$ is defined by

$$\omega_j = \frac{1}{\sqrt{L_v C_j}}. \tag{26}$$

The inductive coupling coefficient is

$$k^2 = \frac{M^2}{L_v L_t}. \tag{27}$$

C_j is the junction capacitance at the operating bias voltage, and Q_v is the varactor Q at the same bias voltage

$$Q_v = \frac{1}{\omega_0 C_j R_s}. \tag{28}$$

It is now possible to design the circuit in Fig. 3(b) so that the frequency jumps will be prevented by forcing (24) to be an equality (loop almost touching the real axis). The other two equations for selection of natural frequencies, as before, are (21) and (22). The numerical solution of the three equations for $Q_v = 10$ and $\alpha = 0.5$ is shown in Fig. 8. It is interesting to mention that no solution can be found for S_{n0} outside the range shown in Fig. 8. Thus, for a given value of Q_v, there exists a limited range of sensitivities which permit the linearization of the modulation curve simultaneously with the condition that tuning be continuous.

When Ω_1, Ω_2, and Ω_3 are substituted in (7), it is possible to compute the modulation curve for the natural frequencies that satisfy (21) and (22), and the equality in (24). The results are shown in Fig. 9. Note that the curves are U-shaped, and no longer S-shaped since $C_3 \neq 0$. However, the continuous tuning of the osc–mod is now assured by the fact that the loop of the impedance Z_{i1} is positioned below the real axis.

The curves in Fig. 9 present the theoretical performance limits which one can hope to approach in practice using two coupled microwave resonators and satisfying the condition of continuous tuning. The corresponding relative bandwidths for 1-percent nonlinearity are summarized in Table I. As an example, curve B ($S_{n0} = 0.02$) shows that the sensitivity departs for less than 1 percent from its

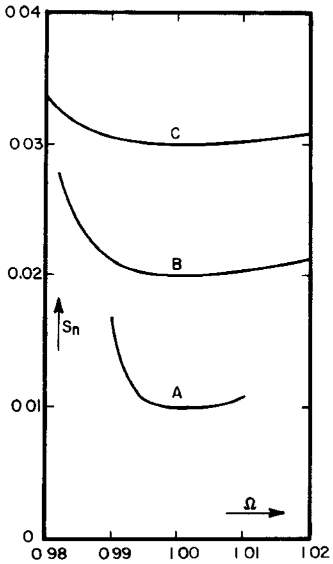

Fig. 9. Normalized modulation curves for the natural frequencies from Fig. 8. Curve A: $S_{n0} = 0.01$, Curve B: $S_{n0} = 0.02$, Curve C: $S_{n0} = 0.03$.

nominal value over the relative bandwidth of 0.0108. Thus, for a varactor having $\alpha = 0.5$ and $Q_v = 10$, $V_b = 10$ V, $\phi_c = 0.7$ V, operating at $f_0 = 2$ GHz, the sensitivity of $S = 0.02 \cdot 2000/10.7 = 3.7$ MHz/V can be maintained within 1-percent limits in a bandwidth of $0.0108 \cdot 2000 = 21.6$ MHz.

VI. Application

The guidelines summarized in Fig. 9 were applied in the development of the osc–mods used in a new generation of analog microwave radios [12]. The discussion of the actual circuits is outside the scope of this paper. It was found, however, that although lumped-element models were used, the guidelines were also applicable to distributed circuits. This is to be expected since the only difference between the two types of circuits is the presence of poles and zeros above the pole-zero configuration chosen for the osc–mod. These higher frequency poles and zeros usually have only a minor effect on the linearity.

VII. Conclusions

An expression for the modulation curve has been derived for a lossless two-port tuning circuit model. The requirements $C_2 = C_3 = 0$ in the Taylor series expansion of the modulation curve leads to an optimum selection of resonant frequencies Ω_1, Ω_2, and Ω_3, which are then used to synthesize the tuning circuit. The resulting modulation curve is S-shaped. For a circuit consisting of two coupled resonators, the requirement for continuous tuning is used in place of the condition $C_3 = 0$. Using this requirement, new values of resonant frequencies Ω_1, Ω_2, and Ω_3 were computed. The corresponding modulation curves are now U-shaped, and the bandwidth is approximately one-half that of the ideal. Limits of modulation bandwidth were tabulated for 1-percent linearity for the ideal and practical cases.

Except for the case of the osc–mod circuit containing a single resonator, there is no evidence that hyperabrupt varactors offer any advantages over conventional abrupt varactors, as far as linearity of the modulation curve is concerned.

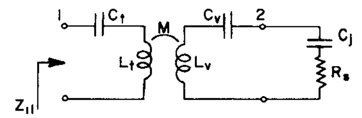

Fig. 10. Two-port from Fig. 3(b) terminated in a varactor consisting of R_s and C_j.

Appendix

When port 2 of the osc–mod is terminated by a varactor consisting of the resistance R_s and capacitance C_j as shown in Fig. 10, the input impedance Z_{i1} becomes

$$Z_{i1} = j\omega_2 L_t \beta_2 + \frac{(\omega M)^2}{R_s + j\omega_l L_v \beta_l}. \qquad \text{(A1)}$$

ω_l is defined by (25) and ω_2 is given by

$$\omega_2 = \frac{1}{\sqrt{L_t C_t}}. \qquad \text{(A2)}$$

β_l and β_2 are functions of frequency as follows:

$$\beta_l(\omega) = \frac{\omega}{\omega_l} - \frac{\omega_l}{\omega} \qquad \text{(A3)}$$

$$\beta_2(\omega) = \frac{\omega}{\omega_2} - \frac{\omega_2}{\omega}. \qquad \text{(A4)}$$

In the vicinity of frequency ω_l, β_l is a fast-varying function, whereas β_2 is a slow-varying function of ω. In order to find the point ω_m at which the slope of Z_{i1} is horizontal (see Fig. 7), an approximation can be made that β_2 is constant and only β_l is variable. Then, the frequency ω_m is found from

$$\omega_m \simeq \omega_l\left(1 - \frac{1}{2Q_l}\right) \qquad \text{(A5)}$$

where Q_l is defined as

$$Q_l = \frac{C_j + C_v}{\omega_l R_s C_j C_v}. \qquad \text{(A6)}$$

Since $Q_l \gg Q_v$, we have $\omega_m \simeq \omega_l$. At this frequency, the imaginary part of the impedance Z_{i1} in (A1) is approximately given by

$$X_{i1}(\omega_m) = \omega_2 L_t \beta_2(\omega_m) + \frac{1}{2}\omega_l L_t Q_l k^2. \qquad \text{(A7)}$$

The loop will be situated below the imaginary axis when $X_{i1}(\omega_m) \leq 0$. From this condition, one obtains the following (using $\omega_m \simeq \omega_l$):

$$\omega_2\left(\frac{\omega_l}{\omega_2} - \frac{\omega_2}{\omega_l}\right) + \frac{1}{2}\omega_l Q_l k^2 \leq 0. \qquad \text{(A8)}$$

From (25), (26), (28), and (A6), it is possible to express Q_l in terms of Q_v as follows:

$$Q_l = Q_v \frac{\omega_0 \omega_l}{\omega_j^2}. \qquad \text{(A9)}$$

Substituting (A9) into (A8), one obtains (24).

Acknowledgment

The authors wish to express their appreciation to Dr. F. Ivanek for his stimulation of this work, and for his critical reading of the manuscript.

References

[1] M. I. Grace, "Varactor-tuned avalanche transit-time oscillator with linear tuning characteristics," *IEEE Trans. Microwave Theory Tech.*, vol. MTT-18, pp. 44–45, Jan. 1970.

[2] A. S. Tager and A. D. Khodrevich, "Impatt diode oscillators with electrical frequency tuning and multidiode oscillators," *Radio Eng. Electron. Phys.*, vol. 14, no. 3, pp. 438–442, 1969.

[3] T. Yamashita and M. Okubo, "Frequency modulator using solid device oscillator and varactor," *Fujitsu Scientific & Technical J.*, pp. 1–19, Sept. 1971.

[4] I. Haga, K. Tamura, K. Sakamoto, S. Aihara, and M. Igata, "A reflection type cavity controlled oscillator and a cavity controlled frequency modulator," *NEC Res. Devel.*, no. 36, pp. 75–100, Jan. 1975.

[5] M. J. Howes and D. V. Morgan, Eds., *Variable Impedance Devices.* Chichester: Wiley-Interscience, 1978, ch. 5.

[6] J. Bravman and J. Frey, "High performance varactor tuned Gunn oscillators," *Cornell Elec. Eng. Conf.*, pp. 335–339, Aug. 1971.

[7] C. S. Aitchison and R. V. Gelsthorpe, "A circuit technique for broadbanding the electronic tuning range of Gunn oscillators," *IEEE J. Solid-State Circuits*, vol. SC-12, pp. 21–28, Feb. 1977.

[8] M. Dydyk, "A step-by-step approach to high-power VCO design," *Microwaves*, vol. 18, pp. 54–65, Feb. 1979.

[9] I. Haga, S. Aihara, and M. Mizumura, "6 to 12 GHz band microwave transistor frequency modulator," *NEC Res. Devel.*, no. 52, pp. 64–71, Jan. 1979.

[10] E. Marazzi and V. Rizzoli, "The design of linearizing networks for high-power varactor-tuned frequency modulators," *IEEE Trans. Microwave Theory Tech.*, vol. MTT-28, pp. 767–773, July 1980.

[11] K. Kurokawa, "Some basic characteristics of broadband negative resistance oscillator circuits," *Bell System Tech. J.*, vol. 48, pp. 1937–1955, July–Aug. 1969.

[12] F. Ivanek, "A new generation of medium-capacity microwave radio," *Microwave J.*, vol. 26, pp. 79–89, Aug. 1983.

Darko Kajfez (SM'67) was born in Delnice, Yugoslavia, in 1928. He received the electrical engineer's degree (Dipl. Ing.) from the University of Ljubljana, Yugoslavia, in 1953, and the Ph.D. degree from the University of California, Berkeley, in 1967.

Between 1950 and 1963, he worked in different R&D laboratories in Yugoslavia, primarily in microwave links and radars. From 1963 to 1966, he was a Research Assistant at the Electronics Research Laboratory, University of California, Berkeley, investigating antennas for circular polarization and their feeding circuits. In 1967, he joined the University of Mississippi, where he is now a Professor of Electrical Engineering. During the academic year 1976–1977, he was a Visiting Professor at the Fakulteta za Elektrotehniko, University of Ljubljana, Yugoslavia. His research and teaching interests are in electromagnetic theory and its applications to microwave circuits and antennas.

Eugene J. Hwan (M'65) received the engineer's degree in 1960 from the Bandung Institute of Technology, Indonesia, and the M.S. degree in electrical engineering in 1966 from the University of California, Berkeley.

From 1960 to 1964, he worked at Siemens and Halske, Munich, Germany, in the field of communication systems. He was a Research Assistant at the Electronics Research Laboratory, University of California, from 1965 to 1966. In 1966, he joined Aertech Industries working on microwave components and subsystems. Since 1973, he has been with the Farinon Division, Harris Corporation, where his responsibilities include development of frequency modulated oscillators, low-noise oscillators, and subsystems.